
Article:
Silalahi, Imelda Hotmarisi, Prokhorov, Anton M., Tanner, Theo et al. (3 more authors) (2022) The liquid-crystalline and luminescence properties of polycatenar diphenylpyridine complexes of Palladium(II). JOURNAL OF ORGANOMETALLIC CHEMISTRY. 122455. ISSN 0022-328X

https://doi.org/10.1016/j.jorganchem.2022.122455

Journal of Organometallic Chemistry 977 (2022) 122455

Contents lists available at ScienceDirect

Journal of Organometallic Chemistry

journal homepage: www.elsevier.com/locate/jorganchem

The liquid-crystalline and luminescence properties of polycatenar diphenylpyridine complexes of Palladium(II)

Imelda Hotmarisi Silalahi[a,b], Anton M. Prokhorov[a], Theo Tanner[a], Stephen J. Cowling[a], Adrian C. Whitwood[a], Duncan W. Bruce[a,*]

[a] Department of Chemistry, University of York, Heslington, York YO10 5DD, UK
[b] Department of Chemistry, University of Tanjungpura, Jalan Prof. H. Hadari Nawawi, Pontianak 78124, Indonesia

ARTICLE INFO

Article history:
Received 27 April 2022
Revised 23 June 2022
Accepted 15 July 2022
Available online 20 July 2022

ABSTRACT

Palladium complexes of polycatenar 2,5-diphenylpyridine ligands were prepared in a two-stage reaction from $(NH_4)_2[PdCl_4]$; their liquid crystal and emission properties are reported and discussed. For tetracatenar and hexacatenar derivatives, neither the ligand nor their complexes were liquid crystalline. The tricatenar ligand only showed a SmC phase identified by a Schlieren texture. Palladation of the tricatenar and dicatenar ligands led to complexes showing a SmA phase, with a range that depended on the ligand. The identity of the mesophases was supported by small angle X-ray scattering (SAXS). All ligands and complexes exhibited luminescence properties with the emission lifetimes of the complexes suggesting the absence of phosphorescence.

1. Introduction

The group 10 elements, palladium and platinum in particular, are some of the most commonly found in metallomesogens [1,2]. This is primarily on account of their square-planar geometry in the +2 oxidation state, which makes them amenable to the formation of anisotropic complexes, although there are examples of metallomesogens based on higher coordination numbers such as platinum(III) [3] and platinum(IV) [4–6]. Most recently, platinum(II) complexes in general have attracted attention as many are capable of exhibiting room-temperature phosphorescence and so they have been seen as candidate OLED emitters [7,8]. Of these, cycloplatinated complexes are found to show high luminescence quantum yield in solution and one of the interesting developments has been of the simultaneous incorporation of liquid crystal properties; such materials have recently been reviewed [9]. In most cases, the analogous complexes of palladium can be prepared and are liquid crystalline, but in general they are not emissive owing to the relative high energy of de-energising *d-d* states.

Thus, for example, the complexes in Fig. 1 are of palladium and platinum, and while all of the complexes luminesce at 77 K, only the platinum complexes luminesce in solution. The mesophases shown by these materials depend on the number of chains on the β-diketonate ligand [10].

Several other related palladium(II) complexes have been prepared, notably by the group in Calabria, but while they were able to realise examples of fluorescent complexes, it seemed that intersystem crossing was less inefficient inasmuch as room-temperature triplet emission was absent [11–14].

Some of the most efficient platinum(II) emitters were published by Bruce and co-workers [15,16] who complexed 2,5-diphenylpyridine ligands *via* orthometallation forming complexes with ancillary β-diketonate ligands. (Fig. 2). Related oligomeric derivatives were found to show polarised emission [17].

The 2,5-di(4-alkoxyphenyl)pyridine ligands used in this chemistry were not synthesised using metal-catalysed cross-coupling methodology, rather an intermediate 1,2,4-triazine was prepared by cyclisation. On reaction with norbornadiene, this triazine then eliminated N_2 in a reverse-electron-demand Diels-Alder reaction inserting ethene to give the 2,5-disubstituted pyridine ligand [15]. The flexibility offered by this route [18] allowed for variation of the ligand substitution patterns and, as such, it was possible to design and prepare a series of polycatenar derivatives. The synthesis of these ligands and their complexes with palladium(II) is now described.

* Corresponding author.
E-mail addresses: imelda.h.silalahi@chemistry.untan.ac.id (I.H. Silalahi), duncan.bruce@york.ac.uk (D.W. Bruce).

https://doi.org/10.1016/j.jorganchem.2022.122455

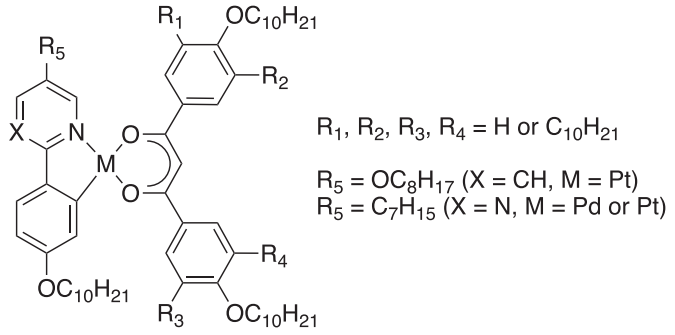

Fig. 1. Mesomorphic complexes of palladium(II) and platinum(II) complexes with 2-phenylpyridine and 2-phenylpyrimidine ligands.

2. Results and discussion

2.1. Synthesis

The ligands were prepared (Fig. 3) based on methods reported by Santoro et al. [15]. The important step in the diphenylpyridine preparation is the synthesis of intermediate 1,2,4-triazine (**5**), which is a condensation reaction between a benzoylhydrazide (**2**) and an α-bromoacetophenone (**4**) in the presence of base. This proceeds in moderate yields of typically between *ca* 45 and 65% depending on the substitution pattern of methoxy groups. The triazine is then converted to the related pyridine (**6**) in an inverse-electron-demand Diels-Alder reaction with norbornadiene, which generates N_2 as a product giving both an enthalpic and entropic driving force. These products are obtained in yields of between *ca* 40 and 80%. The methoxy–substituted diphenylpyridines are then demethylated in high yield in molten pyridinium chloride and the resultant polyhydroxy compounds are alkylated with 1-bromododecane, with the yield of the final product (**8**) decreasing with the increasing number of alcohol groups required functionalisation.

The complexes are then prepared (Fig. 4) by reaction of ligand **8** with ammonium tetrachloropalladate(II) to give the di-μ–chloro complex as a mixture of *cis* and *trans* isomers. The proportions of the two isomers in the mixture was not determined, not least because the product does not depend on the starting isomer. Thus, the dimer is reacted, without purification, with the sodium salt of acetylacetone to give the final product, **9**.

The final ligands and complexes were well characterised through their ^{1}H NMR spectra, which are now discussed for a couple of examples. Thus, the aromatic region of the ^{1}H NMR spectrum of **8b** shows two AMX systems for the central pyridine ring and the ring bearing two alkoxy chains, plus an AA'XX' system for the ring bearing one alkoxy chain. The resonance corresponding to the hydrogen *ortho* to the nitrogen of the central ring is subject to the greatest downfield shift appearing as a doublet with small ^4J coupling of 2.4 Hz at δ = 8.83 ppm. The methylene groups of the chains next to the phenolic oxygens each give rise to a triplet around δ = 4 ppm, but for this compound they overlap to give an apparent multiplet.

Table 1
Summary of X-ray diffraction data for methoxy derivatives of the hexacatenar ligand.

Compound	6d
CCDC Number	2167991
Empirical formula	$C_{23}H_{25}NO_6$
Formula weight/g mol^{-1}	411.44
T/K	110.00(10)
Crystal system	monoclinic
Space group	$C2/c$
a/Å	30.6683(12)
b/Å	5.0752(2)
c/Å	13.3482(6)
α/°	90
β/°	99.941(4)
γ/°	90
Volume/Å [3]	2046.42(15)
Z	4
ρ_{calc} g cm^{-3}	1.335
μ/mm^{-1}	0.798
F(000)	872.0
Crystal size/mm^3	0.22 × 0.18 × 0.12
Radiation/nm	CuKα (λ = 1.54184)
2θ range for data collection/°	11.718 to 142.666
Index ranges	$-37 \le h \le 36, -6 \le k \le 6, -16 \le l \le 15$
Reflections collected	3514
Independent reflections	1932 [R_{int} = 0.0261, R_{sigma} = 0.0363]
Data/restraints/parameters	1932/0/158
Goodness-of-fit on F^2	1.053
Final R indexes [$I >= 2\sigma$ (I)]	R_1 = 0.0391, wR_2 = 0.0978
Final R indexes [all data]	R_1 = 0.0552, wR_2 = 0.1089
Largest diff. peak/hole / e Å^{-3}	0.31/–0.16

The spectrum for **8c** shows three AMX spin systems representing the three chemically inequivalent hydrogens on each ring and once more the resonance corresponding to the hydrogen *ortho* to the nitrogen of the central ring is subject to the greatest downfield shift appearing as a doublet with small ^4J coupling of 2.4 Hz at δ = 8.84 ppm. The resonances associated with the methylene hydrogens bound to the phenolic oxygens, which appear as two simple triplets (δ = 4.12 and 4.05 ppm) of equal intensity corresponding to the two different chemical environments.

In the final complexes, there is some shifting of the position of resonance consequent on complexation and one hydrogen disappears from the metalated ring, giving an AMX spin system for **9b** and an apparently uncoupled AXE system for **9c** ($^5J_{HH}$ is not resolved). In addition, there is a singlet for the methine hydrogen on the acac ligand ($\delta \approx$ 5.4 ppm) and two singlets each of intensity three for the two different methyl groups ($\delta \approx$ 2.1 and 2.05 ppm).

2.2. Single-crystal X-Ray structures

En route to the final ligands, methoxy derivatives (**6**) form part of the synthetic route and for the hexa-substituted variant, it was possible to grow single crystals from acetone (longer chains often mitigate against the formation of good-quality crystals). Crystallographic data are found in Table 1.

The ligand crystallised in the monoclinic space group $C2/c$ and presented an interesting disorder. Thus, there is a centre of inver-

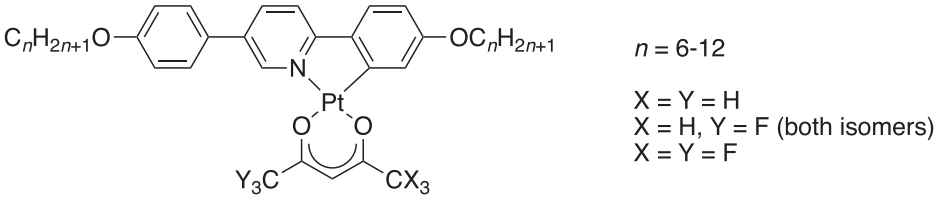

Fig. 2. Luminescent platinum acac complexes of 2,5-di(4-alkoxyphenyl)pyridine. Note that complexes with X = Y = F were neither liquid crystalline nor luminescent.

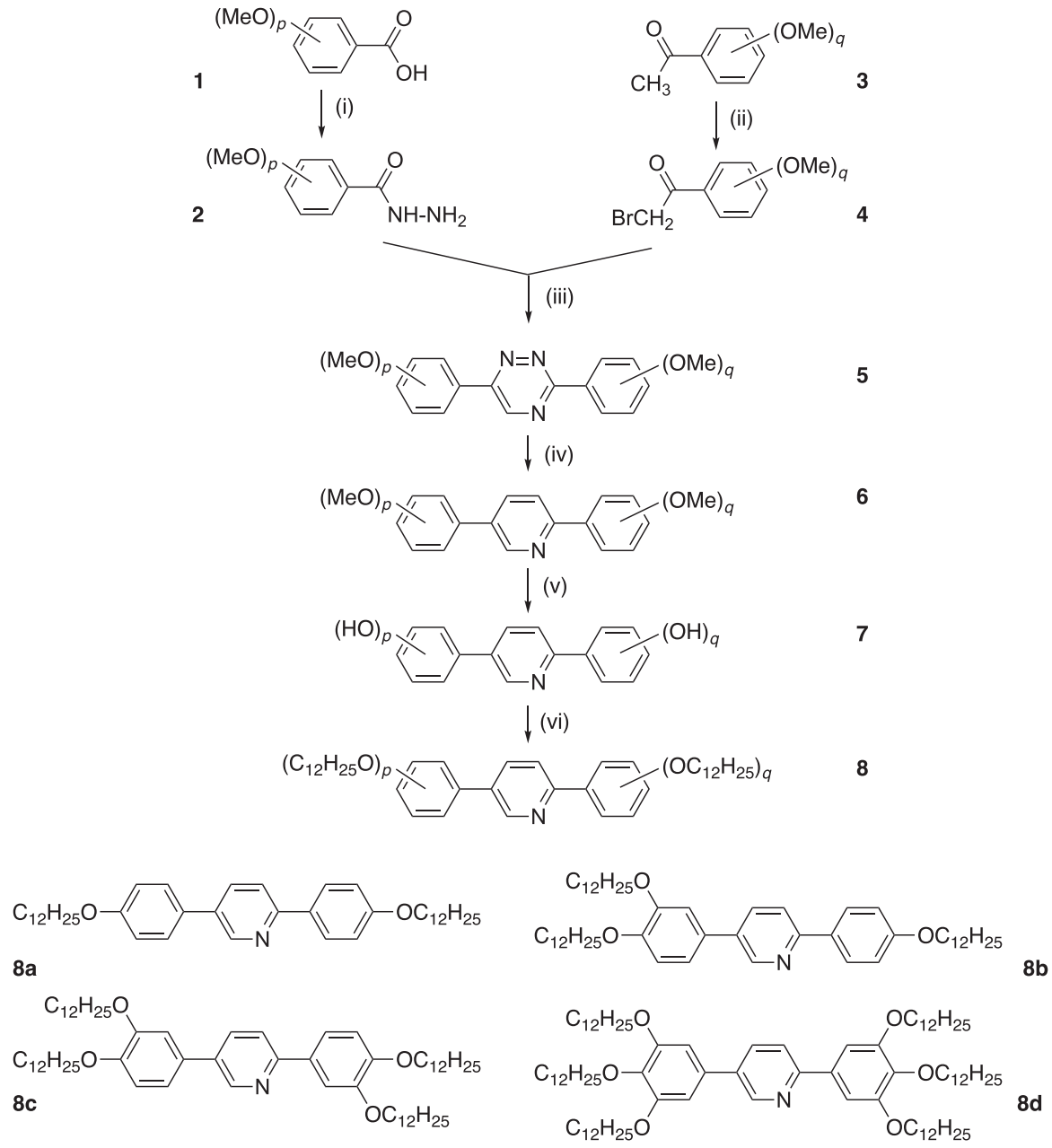

Fig. 3. Preparation of the polycatenar-diphenylpyridine ligands. Conditions: (i) $NH_2NH_2.H_2O$/MeOH, reflux, 17 h; (ii) Br_2/Et_2O; (iii) $NaHCO_3$, EtOH/CH_3COOH, 120 °C, 7 h; (iv) norbornadiene/*o*-xylene, 200 °C, overnight; (v) $[PyH]^+Cl^-$/200 °C, 5 h; (vi) $C_{12}H_{25}Br$/DMF, K_2CO_3, 100 °C, 12 h.

sion in the middle of the central, pyridyl, ring of the molecule, which means that there is half of the molecule in the asymmetric unit. The central ring is then itself disordered about two positions, twisting out of the plane of the molecule so that the planes of the two ring positions make an angle of 59.8° Furthermore, the nitrogen in the centre ring could not be modelled in one position and so a final structure was achieved by modelling all of the disordered ring positions as both C (37.5%) and N (12.5%), to a total occupancy of 50% per position. As such, the images of the individual molecule in Fig. 5 have been 'created' by manipulation in the Mercury software package to 'force' a nitrogen into one position solely for the purposes of illustration. The three rings are not co-planar the plane of the terminal phenyl rings makes an angle of 34.8° to the central pyridyl ring.

The ligands pack in a slipped-stack fashion along the *b*-axis (Fig. 5c) and adjacent stacks are angled towards one another so that the planes defined by the central pyridyl rings in each stack make an angle of 51.7°

2.3. Liquid crystal properties of the ligands and complexes

The thermal behaviour (Table 2) of the ligands and their complexes was investigated by polarising optical microscopy (POM) and differential scanning calorimetry (DSC) thermal analysis and. Ligand **8a** had been reported previously [15] and showed both a SmC and a SmI phase, which on complexation to palladium (**9a**) changes to become a SmA phase. This is directly analogous to the behaviour with platinum and, in common with its mesomorphism,

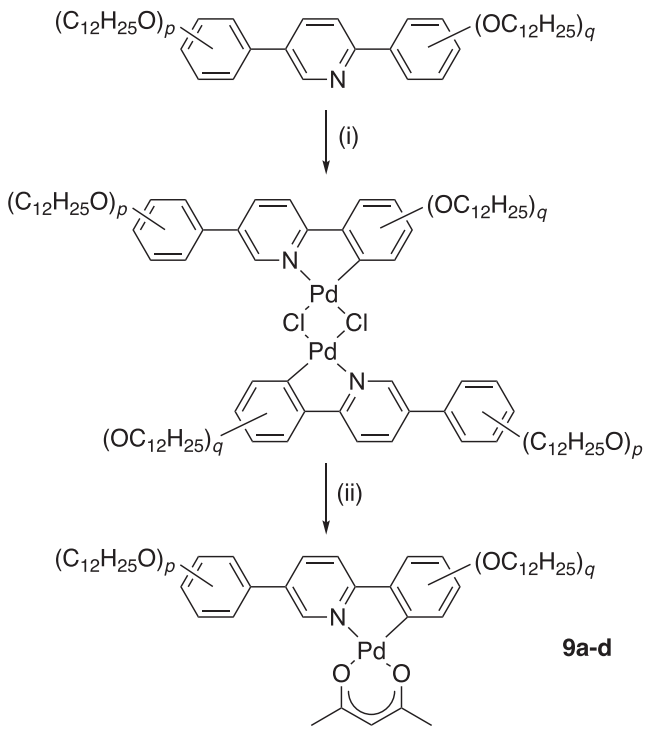

Fig. 4. Preparation of the palladium complexes of the diphenylpyridine ligands. Conditions: (i) $(NH_4)_2[PdCl_4]$/AcOH/100 °C; (ii) Na(acac)/$CHCl_3$-EtOH or acetone/Δ.

Table 2
Thermal behaviour of the compounds.

Compound	Transition	T (°C)	ΔH (kJ mol^{-1})
8a[†]	Cr-SmI	121.7	63.0
	SmI-SmC	171.6	2.4
	SmC-Iso	200.0	18.5
8b	Cr-SmC	92.2	35.0
	SmC-Iso	98.5	4.5
8c	Cr – Iso	106.6	121.5
8d	Cr-Iso	43.3	66.4
9a	Cr-SmA	64.2	1.9
	SmA-Iso	211.3	7.4
9b	Cr-SmA	80.5	4.6
	SmA-Iso	118.9	0.5
9c	Cr-Iso	94.8	47.9
9d	Cr-Iso	44.4	70.3

[†] Reported in ref. 15.

the melting point is raised (to *ca* 160 °C) and the clearing point is enhanced (231 °C for Pt, 211 °C for Pd). Small-angle X-ray data had not previously been collected for this ligand and so the results of this study are shown in Fig. 6 along with unreported optical textures from microscopy for this homologue. The SmC phase (Fig. 6a) gave a single low-angle reflection at $2\theta = 2.56°$ corresponding to a layer spacing of 34.5 Å. From readily available crystal structure data, the calculated length of the molecule, assuming that the chains adopt an all-*trans* arrangement, is 45.9 Å and so if no interdigitation is assumed, then this would represent a tilt angle in the SmC phase of *ca* 41° However, some combination of interdigitation and/or chain folding, which would reduce the effective molecular length, would also reduce the tilt angle and these effects cannot be ruled out. As such, 41° represents a maximum possible tilt angle. Then in the SmI phase (Fig. 6b), there is a small increase in the *Dd*-spacing to 36.27 Å, which would be expected with the formation of a more ordered phase and the increased in-plane order is shown by the sharpening of the wide-angle reflection at $2\theta = 19.69°$ corresponding to a spacing of 4.51 Å (Fig. 6b inset).

Now considering **8b**, the ligand melts at 92 °C to a fluid phase that clears just above 98 °C. On cooling (Fig. 7a), both a broken fan and Schlieren texture are seen, which enables identification as a SmC phase. Formation of a SmC phase is quite typical for tricatenar material of this type, although the limited anisotropy of the core means that the transition temperatures are relatively low and the phase has a fairly narrow range. This is due to the fact that the alkoxy chain in the 3-position is relatively destabilising of the mesophase.

Small-angle X-ray scattering from the SmC phase at 97 °C (Figure S1) shows a single, small-angle reflection at $2\theta = 2.78°$ corresponding to a spacing of 31.8 Å. Given that the maximum length of **8b** is the same as **8a**, then even though the molecules would be expected to pack in an alternating, head-to-tail fashion within the layers to fill space (Figure S2), this would correspond to a tilt angle of some 46° While not impossible, this is quite large and so it is expected that the actual tilt angle is smaller and that there is, in addition, interdigitation and/or chain folding.

For the related palladium complex, **9b**, the SmC phase again disappears to be replaced by a SmA phase, which has a slightly less stable crystal phase (melting at 80.5 °C) and a slightly more stable mesophase (clearing just below 119 °C). The phase was readily characterised by observation of both a focal conic fan texture (Fig. 7c) and a homeotropic arrangement.

Then, no doubt on account of the rather short nature of the molecular core (tetracatenar and more highly substituted materials are normally found with a minimum of four rings in the rigid core), neither the tetracatenar (**8c**) nor the hexacatenar (**8d**) ligand shows a mesophase, both simply melting to the isotropic phase, with a rather low melting point (*ca* 43 °C) observed for **8d** The related palladium complexes also melted at similar temperatures and did not show evidence of liquid crystal behaviour.

The mesophases of the two mesomorphic complexes were also characterised by small-angle X-ray scattering and the diffraction patterns are shown in Fig. 8. Both diffraction patterns show an intense reflection at around $2\theta = 2.5°$, corresponding to spacings of 37.3 Å (**9a**) and 34.6 Å (**9b**). For **9b** there is also a much weaker reflection at $2\theta \approx 5.2°$ corresponding to the $d(002)$ harmonic of the lamellar arrangement and indicating a slightly greater inter-layer correlation. The observed layer spacing for **9a** at *ca* 37 Å is slightly longer than the values found for the free ligand.

2.4. Photophysical properties of the complexes

The photophysical properties of the complexes and ligands were determined in dichloromethane solution at room temperature. The absorption spectra of ligands and complexes are shown in Figs. 9 and 10, whereas the spectra overlaying each complex with its ligand are given in Fig. S3.

In the ligand spectra, one intense band with a weak high-energy shoulder was observed, the intensity of which (Table x) suggests π-π^* transitions. As the number of alkoxy ligand chains increases from the two (**8a**) through three (**8b**) to four (**8c**), the absorption maximum red shifts, almost certainly owing to a destabilisation of the HOMO. However, when the ligand contains six alkoxy chains (**8d**), the absorption wavelength blue shifts so that it was effectively coincident with that of the tricatenar ligand, **8b** and the shoulder did not appear to be present. These changes in λ_{max} can be accounted using Dewar's rules [19].

On complexation, the higher-energy band resolves to a great degree, which is evident for **9a** and better seen for **9b** and **9c**. However, given that there is no shoulder observed for ligand **8d**,

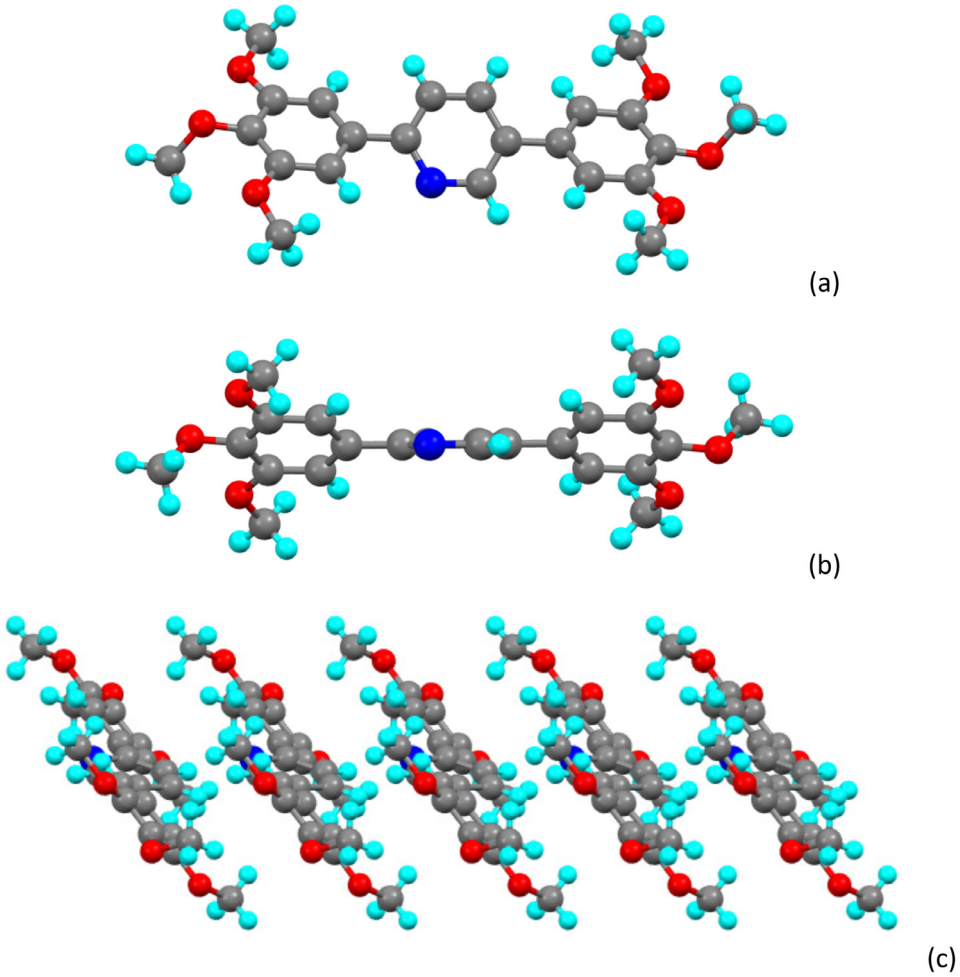

Fig. 5. Two views: a) top-down and b) side-on of the hexacatenar ligand and c) a view of its packing viewed down the *a*-axis. Nitrogen atom 'forced' to appear for the purposes of the diagram – see text.

then it is no surprise that there appears little change in the high-energy absorption on complexation.

The other effect of complexation is the appearance of a longer-wavelength absorption at around 370 nm for **9a** and **9b**, and 400 nm for **9c**, which by analogy with related complexes of platinum(II) is assigned as charge-transfer in nature, derived from orbitals with combinations of ligand and metal character [15]. For **9d** the additional absorption is between these two values at 390 nm, although in this case it is very much less intense. Indeed, with the exception of the weak longer-wavelength absorption, the spectrum of **9d** appears to have changed little from that of **8d** although the absorptivity of the complex increased (Table 3). It is not at all clear why this should be, but as more alkoxy chains are added, so the aromatic system becomes increasingly electron rich, which is likely to act to increase the level of the HOMO. Given that the longer-wavelength absorption that involves metal orbitals, then it could be that the increase in HOMO energy reduces the effectiveness of ligand/metal orbital overlap, leaving the ligand orbitals relatively unperturbed. However, a full understanding would require an extensive computational approach, which is not part of this study.

When excited by light of wavelength 310 to 327 nm, all the ligands and their complexes emit light in the range of 380 to 410 nm, with some red shifting as the number of ligand alkoxy groups increases. Complexes **9a** – **9c** show an additional emission peak at 430–437 nm (**9a, 9b**) or 468 nm (**9c**, weak) when excited at a lower energy (378 nm, 380 and 400 nm for **9a, 9b** and **9c**, respectively). However, such an emission was not observed in the spectra of **9d** (Figure S4 shows spectra for **8c**/**9c**). The emission lifetime of the ligands and the complexes ranges from 0.38 to 1.5 ns, increasing with the number of the alkoxy groups. The relatively short emission lifetime indicates emission from a singlet excited state.

Table 3
Photophysical properties of ligands and complexes in CH_2Cl_2 Solution at 298 K, exciting at the absorption maximum.

	Absorption, λ_{max}/nm($10^3\varepsilon$ / M^{-1} cm^{-1})	Emission, λ_{max}/nm	Lifetime, τ/s (degassed)
8a	310 (72.4), 279 (sh)	380 (Exc. 310)	0.5 ns (380 nm)
8b	318 (38.4), 280 (sh)	390 (Exc. 317)	0.78 ns (390 nm)
8c	325 (31.0), 281 (sh)	390 (Exc. 327)	1.13 ns (390 nm)
8d	319 (33.0)	410 (Exc. 320)	1.5 ns (390 nm)
9a	298 (436.7), 321 (sh), 377 (203.9)	380 (Exc. 298), 430 (Exc. 378)	0.49 ns (380 nm), 0.15 ns (430 nm)
9b	290 (26.7), 321 (25.9), 380 (19.1)	391 (Exc. 300), 437 (Exc. 380)	0.38 ns (437 nm)
9c	293 (90.7), 316 (93.1), 400 (50.2)	391 (Exc. 317), 468 (Exc. 400)	1.15 ns (391 nm)
9d	321 (77.6)	410 (Exc. 320)	1.5 ns (410 nm)

Very weak emission.

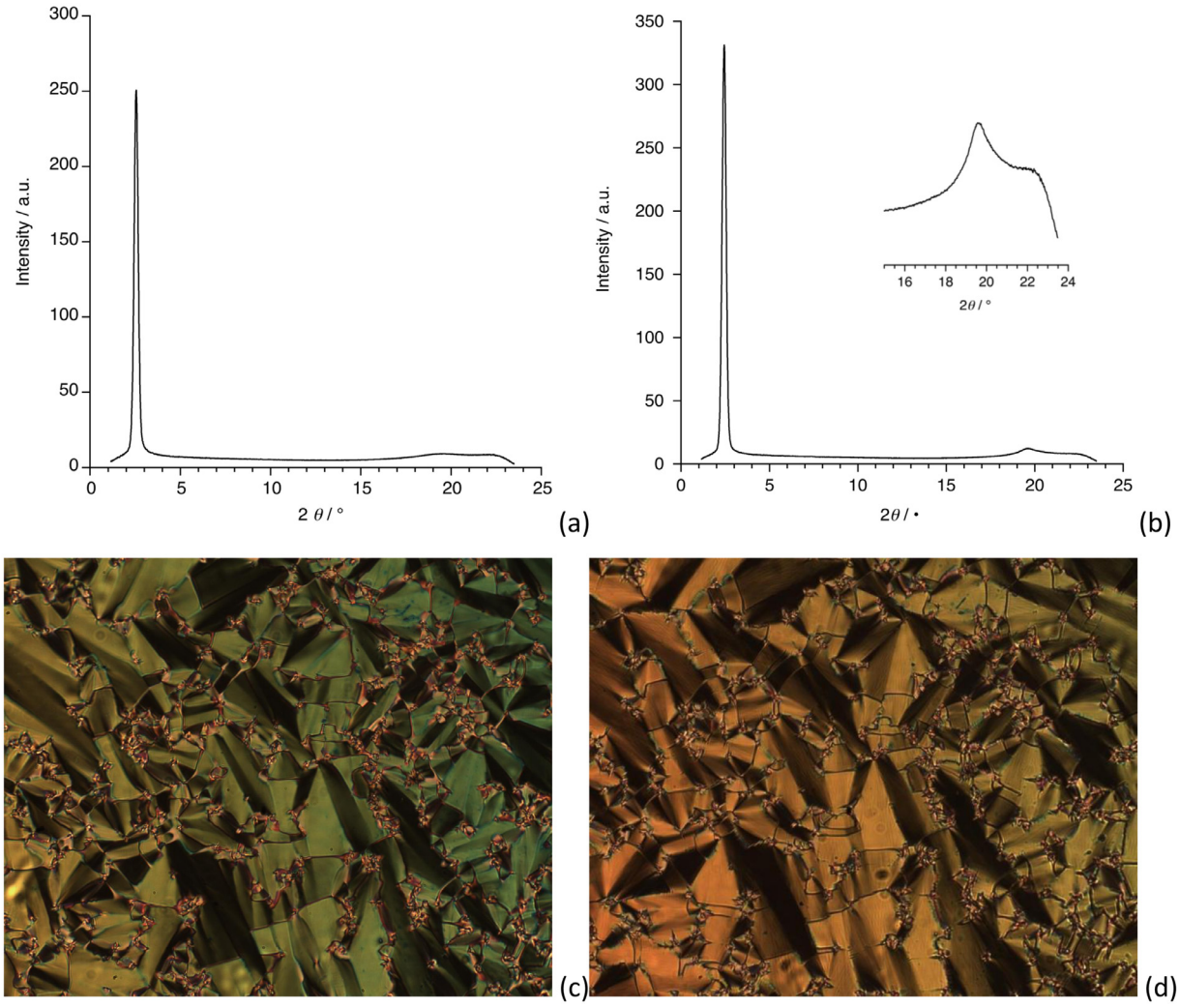

Fig. 6. Small-angle X-ray scattering patterns for **8a** at (a) 195 °C in the SmC phase and (b) 160 °C in the SmI phase, with the inset showing an enlargement of the wide-angle region and optical textures (c) in the SmC phase at 200 °C and (d) in the SmI phase at 167.5 °C. The microscope magnification employed was x200.

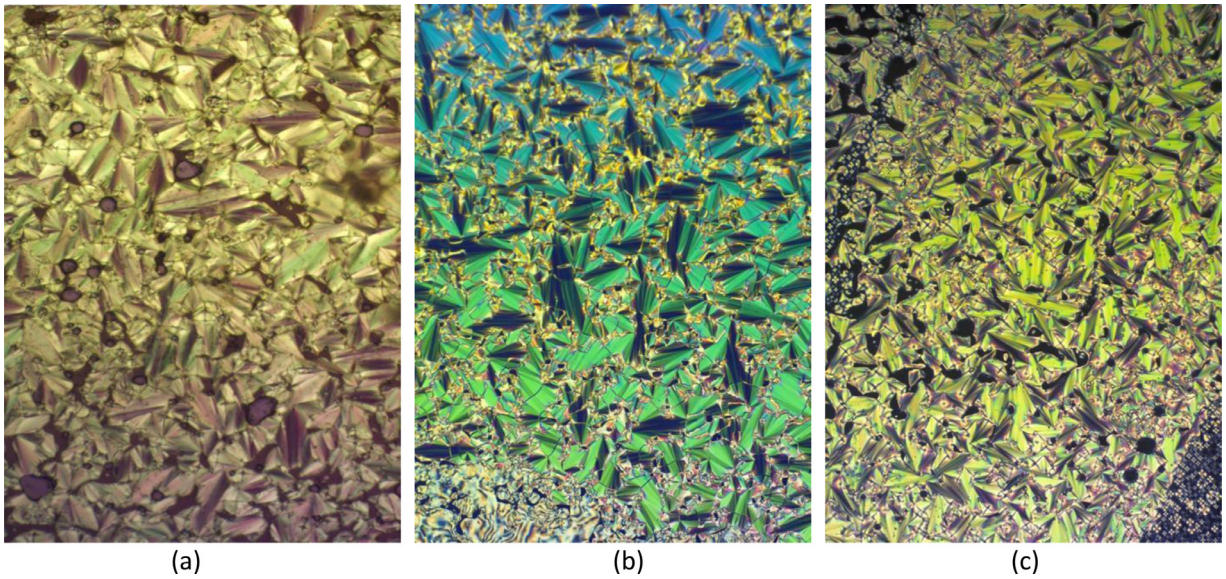

Fig. 7. Optical micrographs (on cooling) of the (a) SmA phase of **9a** at 208 °C; (b) SmC phase of **8b** at 98 °C and (c) SmA phase of **9b** at 105 °C. The microscope magnification employed was x100.

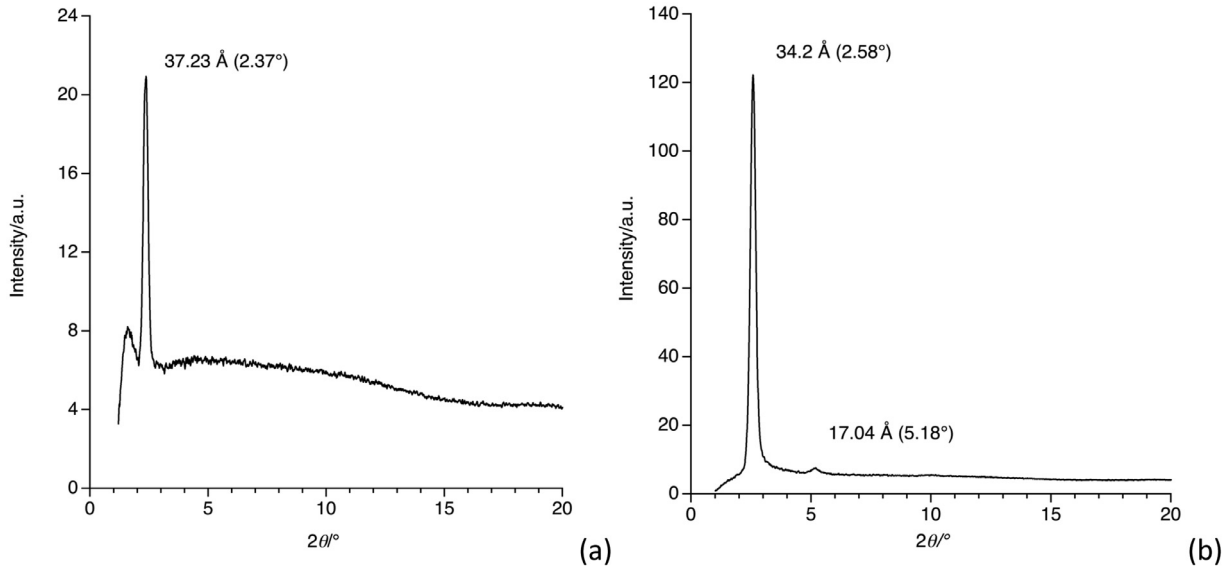

Fig. 8. The small-angle X-ray scattering pattern of (a) **9a** in the SmA phase at 205 °C and (b) **9b** in the SmA phase at 105 °C. Note that the apparent reflection at $2\theta \approx 1.6°$ arises from the beam clipping the beam stop.

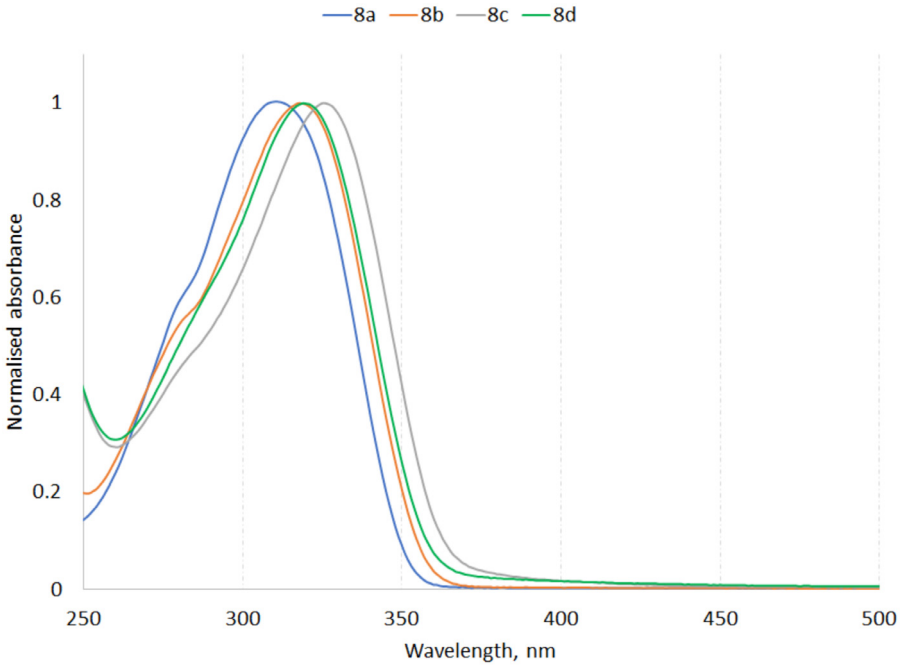

Fig. 9. The normalised absorption spectra of the ligands in dichloromethane solution at room temperature. Solutions were between 1.3 and 2.8 × 10^{-5} mol dm^{-3}.

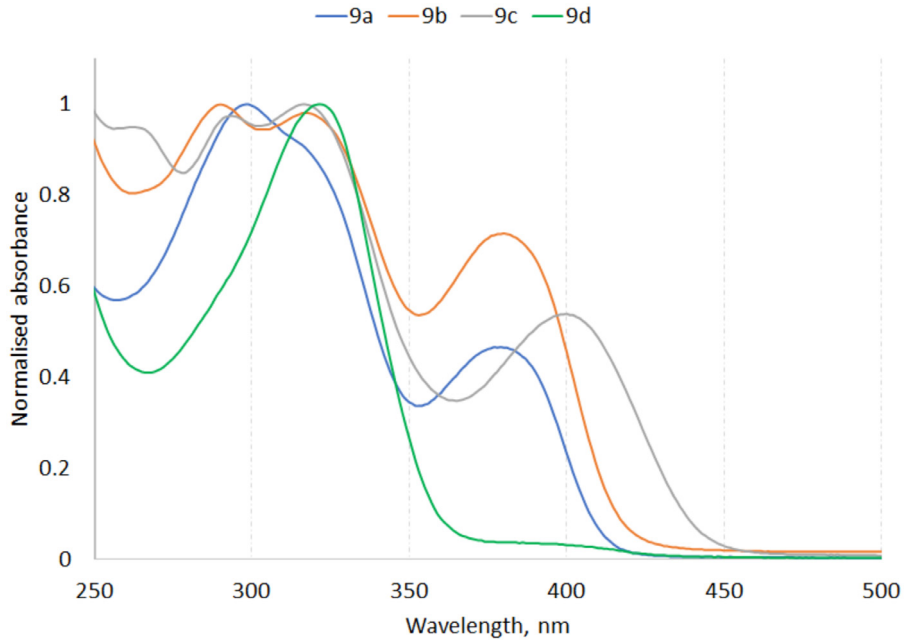

Fig. 10. The normalised absorption spectra of the complexes in dichloromethane solution at room temperature. Solutions were between 0.8 and 2.7 × 10^{-5} mol dm^{-3}.

3. Conclusions

The synthesis and characterisation of metallomesogens of palladium(II) complexes based on polycatenar-diphenylpyridine ligands and acac co-ligand were carried out. In this system where the core mesogens possess three rings, three terminal chains are required to display mesomorphism. For tetracatenar and hexacatenar systems, ligands as well as the complexes showed no liquid- crystallinity. Complexation of the ligands slightly increased the isotropic temperatures although it reduced the anisotropy. The chains play an important role in thermal behaviour. All ligands and complexes exhibited luminescence properties; the complexes emitted light in the range of 430 – 472 nm in addition to the emission that also demonstrated by ligands alone, in the range of 380 – 410 nm with emission lifetimes of 0.38 – 1.50 ns suggesting the absence of phosphorescence.

Declaration of Competing Interest

The authors declare the following financial interests/personal relationships which may be considered as potential competing interests: Imelda Hotmarisi Silalahi reports financial support was provided by Ministry of Education and Culture of the Republic of Indonesia. Theo Tanner reports financial support was provided by University of York. Duncan Bruce & Anton Prokhorov report financial support was provided by Engineering and Physical Sciences Research Council (EP/H006710/1).

Acknowledgements

We thank the EPSRC for support (EP/H006710/1; AMP) and the University of York for a postgraduate studentship (TT). This publication is enabled through a Post-Doctoral Grant (IHS) from the Directorate for Resources, the Ministry of Education and Culture of the Republic of Indonesia.

Supplementary materials

Supplementary material associated with this article can be found, in the online version, at doi:10.1016/j.jorganchem.2022.122455.

References

[1] J. Torroba, D.W. Bruce, Comp. Inorg. Chem. II, Elsevier, Amsterdam, 2013, pp. 837–917. Chapt. 8.21..
[2] B. Donnio, D.W. Bruce, in: J. Dupont, M. Pfeffer (Eds.), Palladacycles, Wiley-VCH, Weinheim, 2008, pp. 239–283. Chpt. 11.
[3] A. Santoro, M. Wegrzyn, A.C. Whitwood, B. Donnio, D.W. Bruce, J. Am. Chem. Soc. 132 (2010) 10689–10691.
[4] R.R. Parker, J.P. Sarju, A.C. Whitwood, J.A.G. Williams, J.M. Lynam, D.W. Bruce, Chem. Eur. J. 24 (2018) 19010–19023.
[5] M. Ghedini, D. Pucci, G. Barberio, Liq. Cryst. 27 (2000) 1277–1283.
[6] M. Ghedini, D. Pucci, A. Crispini, G. Barberio, Organometallics 18 (1999) 2116–2124.
[7] E.V. Puttock, M.T. Walden, J.A.G. Williams, Coord. Chem. Rev. 367 (2018) 127–162.
[8] C. Cebrian, M. Mauro, Beil. J. Org. Chem. 14 (2018) 1459–1481.
[9] X. Wu, M. Zhu, D.W. Bruce, W. Zhu, Y. Wang, J. Mater. Chem. C. 6 (2018) 9848–9860.
[10] T. Hegmann, J. Kain, S. Diele, B. Schubert, H. Bogel, C. Tschierske, J. Mater. Chem. 13 (2003) 991–1003.
[11] D. Pucci, G. Barberio, A. Crispini, O. Francescangeli, M. Ghedini, M. La Deda, Eur. J. Inorg. Chem. (2003) 3649–3661.
[12] M.L. Deda, M. Ghedini, I. Aiello, T. Pugliese, F. Barigelletti, G. Accorsi, J. Organomet. Chem. 690 (2005) 857–861.
[13] M. Ghedini, D. Pucci, A. Crispini, A. Bellusci, M.L. Deda, I. Aiello, T. Pugliese, Inorg. Chem. Commun. 10 (2007) 243–246.
[14] M. Micutz, M. Ilis, T. Staicu, F. Dumitrascu, I. Pasuk, Y. Molard, T. Roisnel, V. Circu, Dalton Trans 43 (2014) 1151–1161.
[15] A. Santoro, A.C. Whitwood, J.A.G. Williams, V.N. Kozhevnikov, D.W. Bruce, Chem. Mater. 21 (2009) 3871–3882.
[16] M. Spencer, A. Santoro, G.R. Freeman, A. Diez, P.R. Murray, J. Torroba, A.C. Whitwood, L.J. Yellowlees, J.A.G. Williams, D.W. Bruce, Dalton Trans 41 (2012) 14244–14256.
[17] A. Diez, S.J. Cowling, D.W. Bruce, Chem. Commun. 48 (2012) 10298–10300.
[18] R.A.A. Foster, M.C. Willis, Chem. Soc. Rev. 42 (2013) 63–76.
[19] M.J.S. Dewar, J. Chem. Soc, in: Nonlinear Optical Properties of Organic Molecules and Crystals, Vol. 1, Chpt. II-3, Academic, London, 1987, pp. 2329–2334. Eds. D. S. Chemla and J. Zyss.